Interaction of Carbon Black Particles and DPPC at the Air/Water Interface: Thermodynamics and Rheology

Eduardo Guzmán,[*,‡] Eva Santini, Dominika Zabiegaj, Michele Ferrari, Libero Liggieri, Francesca Ravera[*]

Consiglio Nazionale delle Ricerche – Istituto per l'Energetica e le Interfasi, UOS Genova (CNR-IENI)

Via De Marini 6, 16149-Genoa (Italy)

[*] To whom correspondence must be addressed: eduardogs@quim.ucm.es (EG) and f.ravera@ge.ieni.cnr.it (FR)

[‡] *Current Address*:

Departamento de Química Física I, Facultad de Ciencias Químicas, Universidad Complutense de Madrid

Ciudad Universitaria s/n, 28040-Madrid (Spain)

Abstract

The interaction of carbon black particles (CB) with 1,2-Dipalmitoyl-sn-glycerol-3-phosphocholine (DPPC) at the water/air interface has been investigated by means of a pool of surface sensitive techniques, in order to analyze the thermodynamic and rheological aspects of these mixed systems. The incorporation of carbonaceous particles to the lipid monolayers induces changes in the surface pressure - area isotherm, as revealed by the shifting to higher surface area of the maximum packing degree of the monolayer, and the decrease of the collapse pressure. These changes are strongly dependent on the DPPC:CB weight ratio at the interface and can be explained by the disruption of the monolayer structure due to the particle incorporation that provokes the modification of the cohesive interactions along the monolayer. Measurements of dilational viscoelasticity against frequency, at different degrees of monolayer compression, have been performed by means of the Oscillatory Barrier method. The rheological response of the monolayer is only slightly affected by the presence of CB, even if a modification of the quasi – equilibrium dilational elasticity, as well as of the frequency dependence of the viscoelastic modulus, is appreciable increasing the particle concentration. Being DPPC the major component of many systems with biological interest (cell membranes, lung surfactant), the results obtained here are expected to contribute to the understanding of the carbon particle interaction with biological relevant systems.

Keywords: Lipids, Nanoparticles, Langmuir monolayers, Interfacial rheology, Toxicity

1. Introduction

The presence of carbon-based particles in the environment has undergone an important growth in the last years, being the combustion processes of fossil fuels in industries, power plants and vehicles the most important sources of these particulate materials.[1,2,3] Recently, the wide spread of nanoparticles is also increasing due to the industrial production of nanostructured materials and, among that carbon based nanomaterials.[4,5,6,7,8] This has driven the development of specific research activities focused on the evaluation of the environmental impact of nanoparticles and their potential risk for health.[9,10,11,12,13]

Several studies are available in literature dealing with the interaction of nano-sized particles of different nature and features with biologically relevant systems, such as lung surfactant and biomembranes.[14,15,16,17,18,19,20,21] Biological relevant interfaces usually present complex supramolecular structures and consist on mixed layers of lipids and proteins,[22] whose principal constituent is the saturated lipid 1,2-Dipalmitoyl-sn-glycerol-3-phosphocholine (DPPC).[23,24,25,26]

Langmuir monolayers of appropriate lipid based mixtures are well-accepted models to investigate the surface properties of biological systems, such as cell membrane and lung surfactants.[27,28,29,30,31] For this reason, investigating the mechanisms of interaction of nanoparticles with these monolayers and the change induced on the behavior and structure of these latest is relevant to understand the potential adverse effects of these materials.

Moreover, it is well established that the interaction of nanoparticles with adsorbed or spread surfactant layers, and their eventual incorporation, may significantly affect the mechanical surface properties of the system, i.e. the interfacial tension and surface rheology. This has been shown in several physical chemistry based studies on nanoparticles of different nature,[32,33,34] and, in particular, on carbonaceous particles.[35,36]

The present work focuses on the effects of carbon nanoparticles on the mechanical and structural properties of a DPPC monolayer. DPPC is probably the most studied lipid in the literature, both from the thermodynamic[37,38,39] and the rheological points of view.[40,41] This great importance is associated with its ability to form monolayers that can reach very low values of surface tensions, due to the formation of condensed phases at physiological temperatures,[41,42,43] which is of great importance for the correct physiological functionality of many organs, tissues and fluids.[27,44]

In recent years, some studies have been already carried out on the effect of carbonaceous nanoparticles on the equilibrium properties of lipid monolayers,[45,46,47,48,49] evidencing the role of the composition and surface nature of the particles.

Aim of this work is to better understand the effect of Carbon Black (CB) particles on the structure and rheological properties of DPPC Langmuir monolayers. Complementary experimental methods have been used such as those utilizing the Langmuir trough, to obtain the compression isotherms and the dilational elasticity of the layers by oscillatory barriers experiments, and the Brewster Angle Microscopy (BAM) to assess the micro structure of the mixed layers during compression. By the combination of these techniques, it has been possible to correlate the effects induced by carbon nanoparticles on the equilibrium and dynamic mechanical properties of the DPPC monolayers, with the modification of their structural features.

2. Materials and Methods

2.1. Materials

1,2-Dipalmitoyl-sn-glycerol-3-phosphocholine (DPPC) was purchased from Sigma (Germany) at 99 % purity and used without further purification. The molecular weight of this lipid is 734.1 g/mol. For the spreading, DPPC was dissolved in chloroform for HPLC from Sigma (Germany).

Carbon Black (CB) used in this work is a commercial sample purchased from Phillips Petroleum Co, whose characterization was performed in a previous work.[50] As evidenced by TEM and AFM analysis CB is composed by chain-like aggregates of spherical primary particles, with average size of 15-29 nm and hydrodynamic diameter of the aggregates of 120 ± 20 nm by DLS. Carbon Black has a density of 1.8 g/cm^3, at 25°C, and the BET specific area of the powder is 51 m^2/g. Being CB nanoparticles hydrophobic, they can be spread on the water surface from dispersions in chloroform.

Water for all the reported measurements was deionized and purified by a multi-cartridge system (Elix plus Milli-Q, Millipore) which provides a resistivity greater than 18 MΩ·cm and a surface tension of 72.5 mN/m without any appreciable kinetics over several hours.

2.2.Methods

The experiments reported in this study have been performed using a Langmuir trough (KSV minithrough, Finland) equipped with two Delrin® barriers allowing for symmetric compression / expansion of the free liquid surface. The total surface area of the Teflon trough is 243 cm^2. The surface tension, γ, was measured through a paper Willhelmy plate (Whatman CHR1 chromatography paper, effective perimeter 20.6 mm, supplied by KSV), ensuring a zero-angle contact angle. Surface pressure, Π, is then obtained as the difference between the surface pressure of the pure water γ_w and γ, i.e. $\Pi = \gamma_w - \gamma$.

The lipid monolayers are spread on the aqueous sub-phase contained in the Langmuir trough by dropping controlled volumes of DPPC in a chloroform solutions at a concentration of 1 g/L (1.36 mM) by a high precision Hamilton syringe. In this way, it is possible to obtain a controlled surface concentration of DPPC, Γ_0, after the evaporation of the solvent. For all the experiments here reported Γ_0 was about 1.68 10^{-10} moles/cm^2, corresponding to an area per molecule of about 98 $Å^2$. To prepare the mixed monolayers, the given amounts of CB particles were spread onto the previously spread DPPC monolayers, using again Chloroform as spreading solvent. This procedure allows achieving the desired DPPC:CB weight ratio at the interface.

For the determination of the compression isotherm, the surface pressure was typically measured while reducing the free area, A, of the monolayer at constant rate. For the experiments here presented the compression rate used was 2 cm^2/min in order to avoid any undesired non-equilibrium effects in the determination of the isotherms. [51] Compression is started after one hour from the solution/dispersion deposition. This time was checked to be enough to ensure the complete evaporation of the solvent and, in the presence of nanoparticle, the achievement of the equilibrium state for the composite layer.

The Langmuir trough is coupled with a Brewster Angle Microscope (BAM), Multiskop, Optrel (Germany), providing the in-situ image acquisition of the layer at different compression state.

To investigate the rheological response of these monolayers at different compression degree, the Langmuir trough was used according to the Oscillatory Barrier which provides the measurement of the dilational viscoelasticity in a frequency range of 1-200 mHz. This method is extensively described elsewhere[32,52,53] and its appropriateness for the rheological

characterization of lipid – nanoparticles mixed systems has been pointed out in our previous studies.[45,54,55] For all the dilational viscoelasticity measurements reported in this work, the amplitude of the area deformation was $\Delta u = 0.01$ which, as checked by appropriate surface pressure measurement, ensures the linearity of the layer response.

For all the experiments the temperature was controlled at a value of 22.0 ± 0.1 °C.

3. Results and Discussion

A preliminary study on the effect of CB particle on the pure water/ air interfaces has been performed using Langmuir trough, measuring the surface pressure during the compression of the surface laden by CB particles alone at initial concentration of 1.2 μg/cm^2.

The results reported in Figure 1 show that surface tension of the layer obtained in this way is not appreciably different from that of pure water, unless the particle layer reaches a highly packed state, that is at CB surface concentration of 3 μg/cm^2. Reducing further the free surface to overcome this critical concentration, the surface pressure starts to steeply increase meaning that the layer is approaching the total coverage of the water surface as evidenced by the BAM images in Figure 1b.

Insert Figure 1

Figure 1: Compression Surface Pressure – Area isotherm, obtained by the Langmuir trough after the deposition of 0.29 mg of CB particles on pure water (a) and BAM images (size = 311 μm x 418 μm) at different values of surface pressure (b).

When CB particles are spread on DPPC monolayers significant effects on the surface pressure – area isotherms are observed, as described in next session. Such effects are essentially driven by the interaction between the CB particles with the hydrophobic tails of DPPC molecules.

As concerns the preparation of the mixed DPPC-CB monolayer, it is important to underline that the spreading of DPPC is firstly executed at the pure water/air interface and the CB is spread after, on the preformed DPPC monolayer. Unlike other works presented in

literature, where the nanoparticle-lipid mixed layers are obtained by spreading a premixed dispersions,[45,47] using this procedure, the interaction between particles and lipid molecules occurs only at the interface, that is a more significant scenario for the simulation of the NP effects on biological interfaces.

3.1. Surface Pressure – Area Isotherms

Figure 1a reports the compression isotherms for the mixed monolayers of DPPC and CB with different weight ratio between the components. These isotherms are important in order to acquire information on the phase behaviour of mixed systems and to understand how particles alter those mechanical and structural characteristics of the DPPC monolayer, relevant for the functionality of the biological lipid layers. The isotherm of pure DPPC, also shown in Figure 2, is in agreement with those previously reported in literature.[37,38,56,57,58,59]

Insert Figure 2

Figure 2. (a) Π-A/A_0 isotherms of Langmuir monolayer for mixture of DPPC and CB at different weight ratio (a) and dependence on the CB weight fraction, x_{CB}, of A/A_0 at given surface pressure (a), of the collapse pressure, Π_c, (c) and of $(A/A_0)_{lim}$ *(d).*

The incorporation of CB particles does not modify substantially the qualitative feature of the compression isotherms of the monolayer which, independently of the CB weight fraction, x_{CB}, show the typical shape found for pure DPPC monolayers with a plateau at surface pressures of about 7.5 mN/m, corresponding to the coexistence of the two liquid-expanded (LE) and liquid-condensed (LC) phases. A noticeable effect is instead observed on the collapse pressure, Π_c, which tends to decrease with x_{CB} increasing (see Figure 2c). Furthermore, the incorporation of CB to the lipid monolayer shifts the isotherm to higher areas per DPPC molecule, being this shifting strongly dependent on the amount of CB at the interface (see Figure 2b).

From these results, it is possible to assume the existence of two different regimes for the effect on the phase behaviour of DPPC monolayers, dependent on two CB concentration regions. For x_{CB} lower than a certain limit value x_{CB}^{lim} (x_{CB}^{lim}~0.2), the increase of x_{CB}

provokes the shifting to higher areas per molecules of the phase behaviour. This may be explained considering that the introduction of CB determines the increase of the interfacial concentration, leading to an earlier lifting-off of the LE phase of the isotherm in comparison to the pure system. Thus, the presence of nanoparticles induces a faster advancement of the isotherm. This allows considering that the nanoparticles take up part of the area available but there are no important interactions between the nanoparticles and DPPC, at least until high degrees of compression of the monolayers. This latter is evidenced from the decrease on Π_c. However, increasing the weight fraction of CB beyond a limit value, x_{CB}^{lim}, the shift from the pure DPPC monolayer isotherm tends to be reduced as evidenced more clearly in Figure 1b reporting the area dependence on x_{CB} at fixed Π-states. This can be explained considering that the deposition of CB takes place onto preformed DPPC monolayers and, above a certain amount of CB nanoparticles, the available interfacial area could be not sufficient for a monolayer distribution. Thus, it is possible that stacks of nanoparticles grow onto the preformed mixed film leading to the formation of folds toward the aqueous subphase in a similar way than that proposed by Lin et al.[60] for PAMAM dendrimers - DPPC systems. This folding of the interfacial layer increases the available area per DPPC molecule.

The qualitative similar behaviour found for the isotherms independently of x_{CB} can be related to the weak hydrophobic interactions between carbon particles and DPPC molecules, which assume an important role only after the mixed layer has reached a high packing density. This is confirmed by the BAM images (Figure 3) obtained in the region of the coexistence plateau where the nucleation and growth of the typical DPPC microdomains around the CB aggregates is observed, independently of the x_{CB}.

Insert Figure 3

Figure 3. BAM images sequences (images size = 311 μm x 418 μm) obtained at *Π=7.5 mN/m,* states for mixed monolayers of DPPC and CB with different DPPC:CB weight ratio.

The micro-domains observed for the mixed DPPC – CB monolayers in the region of the phase coexistence present similar bean-like shape to those observed for pure DPPC[28,41,56]

and their sizes are not strongly modified by the presence of particles. This can be considered a further confirmation of the low influence of the hydrophobic interactions in the local packing of the DPPC molecules. This scenario is different from that found for DPPC with hydrophilic silica nanoparticles where the presence of charged particles in the sublayer, changing the electrostatic environment, affects the shape and dimensions of the domains, modifying the line tension and the hydrophobic mismatch.[61,62] For the highest surface pressure, the monolayers are quasi-homogeneous films with some dispersed carbon aggregates. Comparing these last images with those obtained for pure CB monolayer (Figure 1b), which present massive aggregates of carbonaceous nanoparticles during the whole phase behaviour, one can say that the interaction with the lipid molecules enhances the CB particle dispersion at the air/water interface.

Another important effect associated with the incorporation the CB to the lipid monolayer is the decrease of the collapse pressure, Π_c (see Figure 1c). This is ascribable to the lateral hydrophobic cohesive interactions, occurring along the monolayer at high degree of compression. Thus, it can be expected the existence of strong cohesive interactions between the molecules, when pure DPPC monolayers are considered, that allow forming highly condensed DPPC monolayers with high values of Π_c. However, the incorporation of CB weakens the cohesive interactions between the DPPC molecules due to their inhomogeneous morphology. In other words, the presence of particles induces a certain steric hindrance to the DPPC molecular cohesion in the monolayer and, consequently, reduces the packing at high interfacial concentration.

In order to quantify the steric hindrance in the monolayer packing, an effective parameter is the area limit, $(A/A_0)_{lim}$, estimated by the extrapolation of the steepest, high pressure, linear part of the $\Pi - A/A_0$ curve to zero surface pressure. This quantity provides information about the maximum packing area of the monolayer before the collapse. In Figure 1d it is shown that the packing of the monolayers is reduced (increase of $(A/A_0)_{lim}$) by the incorporation of a small quantity of CB particles, in agreement with the reduction of the cohesion between the DPPC molecules. However, the further increase of x_{CB} leads to a slightly decrease of $(A/A_0)_{lim}$. This can be explained by the stronger packing of the particle at the interface favoured by the many body interactions, which induces an enhancement of the CB particle packing. Even though, the average cohesion of the DPPC molecules always decreases with the increase of x_{CB}.

3.2. Effect of x_{CB} in the Interfacial Miscibility between DPPC and CB

Further information on the interaction between DPPC and CB nanoparticles may be obtained recurring to simple considerations based on the thermodynamic of mixtures.[63] For DPPC-CB particle mixtures, it is possible to define, at each value of the surface pressure, an ideal area of the monolayer per unit weight (or specific area), A_{ideal}, i.e.

$$A_{ideal} = x_{DPPC} A_{DPPC} + x_{CB} A_{CB} \quad (1)$$

where A_{DPPC} and A_{CB} are the specific areas of the monolayers of pure DPPC and CB for the considered surface pressure, Π, and x_{DPPC} and x_{CB} the weight fractions of DPPC and CB, respectively, in the mixed monolayers. The deviation of the mixed monolayer behaviour from that of the ideal mixture the can be evaluated through an excess area, A_{ex}, defined as follows

$$A_{ex} = A_{12} - A_{ideal} \quad (2)$$

where A_{12} is the real area of the mixed monolayer per unit weight measured for the given value of Π.

Notice that for the here studied solid particle – lipid mixture, it is more appropriate to treat the monolayer miscibility in terms of specific area instead of area per molecules as is usually done for multi-component surfactant monolayers.

For the system studied here, A_{ex} can be calculated using the data of the compression isotherms obtained for the mixed monolayers (Figure 2) to evaluate A_{12} and those measured for the pure CB particles and DPPC monolayers (Figures 1 and 2) to obtain A_{CB} and A_{DPPC}, respectively. Figure 4 shows the calculated values of A_{ex} as a function of x_{CB} for different Π values.

Insert Figure 4

Figure 4. A_{ex} dependence on the x_{CB} for different values of the surface pressures.

From the experimental results, it is possible to define two different regimes corresponding to positive and negative values of A_{ex}. In the first one, a growing trend of A_{ex} with x_{CB} is found, pointing out the immiscibility between DPPC molecules and CB. This may be related to the low importance of the hydrophobic interactions between the nanoparticles and the lipids molecules, as was already discussed in previous section. In this region in fact, as evidenced by the shifting of the compression isotherm to higher areas without evident modification of the shape, the particles are expected to occupy the interfacial area without appreciably affecting the cohesion between DPPC and CB. However, the decrease of the value of A_{ex} with the increase of Π observed beyond x_{CB}^{lim}, indicates a larger importance of the hydrophobic interactions between nanoparticles and lipid molecules, with the increasing of the CB density, which consequently enhances the cohesion in the monolayer. Such the global cohesion, however, is lower than that expected for a monolayer of pure DPPC. Increasing x_{CB} beyond 0.5, we observe that A_{ex} becomes negative. This means that the higher interfacial concentration of nanoparticles enhances the many-body interactions, resulting in the miscibility of the monolayer.[64]

3.3. Compression – Expansion Cycle: Effect of the Nanoparticles on the Hysteresis

To deepen the thermodynamic study of these mixed monolayers, their response to quasi-static compression – expansion cycles of the surface area have been investigated. This type of experiments allows for an evaluation of possible hysteresis related to the internal reorganization of the monolayer, formation of multilayers or expulsion of lipid molecules to the subphase and re-spreading processes. This is particularly important in the case of biological fluids, such as the pulmonary surfactant, because related to physiological response during the respiratory cycle.[65] In the present study an hysteresis has been observed for all the investigated systems. This is related to a non-efficient re-spreading, during the expansion, into the interface of the material squeezed-out during the compression step.[66] An example of a compression expansion cycle obtained for a mixed DPPC-CB layer is reported in Figure 4a. In practice, the value of the surface pressure achieved during compression, Π_{compr}, is in general higher than the corresponding one at the same value of the area during expansion, Π_{exp} and the difference, Π_{compr}-Π_{exp}, is higher at higher compression degree of the monolayer. This is related to the squeezing-out of material from the interface during the compression. The time for the re-entrance of this excluded material is longer than the time necessary for the re-expansion of the monolayer,

leading to a non-efficient re-spreading during the expansion cycle and this provokes an absence of matching of the compression and expansion, since the amount of material at the interface during expansion is always smaller than in the compression step.

For the evaluation of the hysteresis, it is useful to use the normalized hysteresis area, HA_n, defined as [12,15]

$$HA_n = \frac{\left[\int_{A_{\min}}^{A_{\max}} \Pi(A)dA\right]_{compr} - \left[\int_{A_{\min}}^{A_{\max}} \Pi(A)dA\right]_{\exp}}{A_{\max} - A_{\min}} \quad (3)$$

where A_{max} and A_{min} are the maximum and minimum area of the compression-expansion cycle. In Figure 5b *HAn* is reported as a function of the composition of the monolayer.

Insert Figure 5

Figure 5. Example of hysteresis cycle obtained for the complete compression – expansion of the mixed DPPC-CB monolayers at x_{CB}=0.04 (a) and calculated Normalised Hysteresis Area versus CB weight fraction.

In agreement with the observed behavior for the phase diagram, the hysteresis of the compression – expansion cycles shows a strong dependence on the value of x_{CB}. For $x_{CB} < x_{CB}^{lim}$, the hysteresis area increases with x_{CB}. This may be ascribed to an inhomogeneous distribution of the components within the monolayer, which implies an important role of the bidimensional redistribution of the material on the equilibration. For $x_{CB} > x_{CB}^{lim}$, the higher cohesion of the molecules at the interface due to the higher interfacial concentration, allows one to consider negligible the bidimensional reorganization of the material within the monolayers during the re-equilibritation process. Furthermore, this stronger cohesion leads to a reduction of the amount of material squeezed-out from the interface and consequently of the hysteresis area.

From these compression - expansion experiments, it is possible to conclude that the incorporation of particles on the monolayer affects significantly the dynamic of re-entrance of material during the re-expansion process.

3.4. Low Frequency Rheological Measurements

From the Π - A isotherms, it is possible to determine the dilational elasticity under quasi-static compression of the surface area, ε_0. This is related to the elastic energy stored by the monolayer under compressions at constant rate, and provides information on the rigidity of the monolayer upon quasi-static dilation deformation. [67,68,69] For isothermal compression in the Langmuir trough, this quasi-equilibrium dilational elasticity can be written as

$$\varepsilon = -A\left(\frac{\partial \Pi}{\partial A}\right)_T \tag{4}$$

and can be evaluated by the numerical derivative of the Π - A isotherms. In Figure 6, ε_0 obtained for the different mixed monolayers here investigated is reported as a function of the surface pressure.

Insert Figure 6

Figure 6. (a) Quasi-equilibrium dilational elasticity calculated from Π-A isotherms for the mixed monolayers with different values of x_{CB}. (b) Dependence on x_{CB} of the maximum value of ε_0 for the LE and LC phases.

For pure DPPC, the behavior of ε_0 against the surface pressure presents two maxima. The small maximum at low surface pressure corresponds to the elasticity of the LE phase which is characterized by an intrinsic disorder. It is followed, during compression, by a minimum of quasi zero elasticity due to the LE-LC coexistence phase. The second maximum is observed at high surface pressures and presents values of elasticity higher than those of the LE phase. This is attributed to the formation of highly ordered LC phase. The coexistence region of DPPC monolayers presents a quasi-null value of elasticity which is typical of phase coexistences.

As shown in Figure 5a, the incorporation of CB particles does not modify the qualitative feature of the elasticity. However, the maximum of the LC phase is observed for lower values of Π with the increase of the x_{CB}. This is due to the fact that the introduction of particles increases the total interfacial concentration (DPPC + particles). This leads to a prior packing of the monolayer (lower values of Π) and to the subsequent shifting of ε_0 to

lower values of surface pressure. Focusing in the values of the elasticity, when the LE phase is considered it is not observed any change in the values than can be a consequence of the intrinsic disorder of this phase due to the low importance of the van der Waals cohesive interaction between the lipid tails. On the other side, a strong decrease of the values of ε_0 corresponding to the LC phase, is observed increasing x_{CB}. This is related to the formation of composite layers where the cohesive van der Waals interactions between the lipid molecules are reduced. Note that, as discussed above, the increase on x_{CB} makes increasingly important the cohesive interaction between particles and between particles and lipid molecules, but the average cohesion at the interfacial layer is weaken.

In order to deepen the effect of the incorporation of CB particles in the DPPC monolayers, a study of the frequency dependence of the modulus of dilational viscoelasticity for the mixed layers has been performed using the oscillatory barrier method[52,53] at different degree of compression of the monolayers. This kind of experiments allows the relaxation processes with characteristic frequencies within the investigated frequency range to be evidenced by fitting appropriate theoretical curves to the experimental data.[70]

The modulus of the dilational viscoelasticity, $|E|$, against frequency obtained for DPPC-CB monolayers with different x_{CB}, for different values of the reference Π, are reported in Figures 7. Notice that the rate of the surface deformation, $du/dt = (dA/dt)/A$, for the quasi-static experiments discussed above is of the order of 10^{-5} Hz, for all the investigated systems. This rate can be identified with the area perturbation frequency and these ε_0 data associated to that frequency.

Insert Figure 7

Figure 7. Modulus of the dilational viscoelasticity against frequency obtained by oscillatory barrier experiments for mixed monolayers with different values of x_{CB}, at different values of surface pressure, corresponding to different aggregation states. (a) x_{CB} = 0. (b) x_{CB} = 0.09. (c) x_{CB} = 0.33. (d) x_{CB} = 0.75. Lines represent the best fit theoretical curves according to eq. (5).

The results show a dependence of the modulus of the dilational viscoelasticity on the deformation frequency that is well described using a theoretical expression corresponding

to the case of one dynamic relaxation process occurring within the insoluble interfacial layer, [54,70]

$$|E| = \sqrt{\frac{E_1^2 + E_0^2 \lambda_1^2}{1 + \lambda_1^2}} \quad (5)$$

where $\lambda_1 = \nu_1/\nu$ and ν_1 are referred to the characteristic frequency of the process. The best fitting curves to Eq. (5) for the different monolayers are reported in Figures 7. Figure 8 shows the parameters obtained from the modelling of the experimental data to the Eq. (5). As general trend, the introduction of nanoparticles modifies the elasticity limits, E_0 and E_1, and the characteristic frequency of the dynamic process. However, no evidence of additional relaxation processes induced by the introduction of particles was found.

Insert Figure 8

Figure 8. Parameters obtained from the fitting of the rheological experiments of Figure 6 according to eq.(5). The different symbols indicate different values of x_{CB}: (●) x_{CB} = 0. (○) x_{CB} = 0.09. (▼) x_{CB} = 0.33. (Δ) x_{CB} = 0.75.

The incorporation of CB to DPPC monolayers leads to the appearance of a relaxation process with $\nu_1 \sim 10^{-2}$ - 10^{-3} Hz for $\Pi \sim 3$ mN/m. This process was not observed in the absence of particles, at least in the analyzed frequency range, and may be ascribed to rearrangements of the nanoparticles along the interface. When the compression degree of the monolayers increases ($\Pi \sim 6$ and 7.5 mN/m), a kinetic process with $\nu_1 \sim 10^{-3}$ - 10^{-4} Hz is observed independently of the presence or absence of particles at the interface. This is related to the nucleation of LC domains in the LE matrix. The origin of this process is the dynamic exchange of material between the LC phase and the LE matrix. Increasing Π, dynamics processes with $\nu_1 \sim 10^{-4}$ Hz are presented in the whole phase diagram, both for the pure DPPC monolayer and for the mixed monolayer. These relaxations may be related to general rearrangements of the DPPC domains, being attributed in the mixed monolayers to more complex rearrangements, involving the CB particles and the lipid molecules.

The study of the dilational response of DPPC:CB mixed monolayers points out that the introduction of CB only slightly affects the rheological behaviour in the linear regime,

even though differences are observed in the characteristic frequencies of the surface processes. This can be explained considering that the incorporation of CB, as well-distributed inclusions within the monolayer, only modified locally the local structure of DPPC monolayers, Thus, the average rheological response of the monolayer against a small area perturbation does not change significantly due to the local presence of carbon aggregates within the monolayer. Additionally, the evaluation of the dependence of E_0 and E_1 on x_{CB} for fixed values of Π confirms that the introduction of CB slightly reduces the Π of transition between the different phases, evidencing that the CB particles take up part of the interfacial area and induce a prior packing of the monolayer.

4. Conclusions

In this work, the effect of the incorporation of CB nanoparticles on the behaviour of DPPC monolayers has been investigated, focusing both on the equilibrium and dynamic aspects. The coupling of the Langmuir trough technique with BAM has allowed evaluating the impact of carbon particles on the phase behavior, both from the thermodynamic and structural point of view, and the rheological properties of the lipid monolayers.

From the results here obtained one can conclude that carbon particles appreciably affect the properties of DPPC monolayers. These modifications are essentially driven by the interaction between the particles and the hydrophobic tails of the lipid molecules at the interface which can lead to the disruption of the interfacial structure and, consequently, to a modification of the equilibration mechanisms within the monolayer.

The particles may have multiple effects. Besides an increase of the structural disorder of the monolayer a modification of the available free water-air interface is observed for the lipids, together with a possible impoverishment of the surface amount of lipid molecules due to the folding of the interfacial layer. These phenomena have important consequences on the system behavior, as it has been quantitatively shown by measuring the $\Pi - A$ isotherms during compression-expansion cycles, the quasi-equilibrium dilational elasticity and the dynamic behavior. The variation of the properties is strictly dependent on the added amount of particles, as pointed out by the definition of different regions of behavior for the mixed monolayers.

Concluding, even if the DPPC here used is a rather rough model of real biomembranes and biofluids, some information on the possible mechanisms of modification can be applicable to the real biological relevant systems. For this reason, the results contained in this work, are expected to contribute to the understanding, on a more fundamental basis, of the potential toxicological effects of the particulate materials.

Additionally, the observed effects could be utilized as criteria to discriminate potential adverse effects of particles on the physiological function of these systems.

Acknowledgements

This work was financially supported by IIT – Istituto Italiano di Tecnologia within the Project SEED 2009 "Nanoparticle Impact of Pulmonary Surfactant Interfacial Properties – NIPS", and by European Science Foundation, ESF-COST Actions CM1101 and MP1106.

Reference

[1] Kittelon, D.B. Engines and Nanoparticles: A Review. *J. Aerosol. Soc.* **1998**, *29*, 575-588.

[2] Morawska, L.; Bofinger, N.D.; Kocis, L.; Nwankwoala, A. Submicrometer and Supermicrometer Particles from Diesel Vehicle Emissions. *Environ. Sci. Technol.* **1998**, *32*, 2033-2042.

[3] Barnoud, J.; Urbini, L.; Monticelli, L. C60 fullerene promotes lung monolayer collapse. *J. R. Soc. Interface* **2015,** *12*, 20140931.

[4] Nakamura, E.; Isobe, H. Functionalized fullerenes in water. The first 10 years of their chemistry, biology, and nanoscience. *Acc. Chem. Res.* **2003**, *36*, 807-814.

[5] Zabiegaj, D.; Santini, E.; Ferrari, M.; Liggieri, L.; Ravera, F. Carbon based porous materials from particle stabilized wet foams. *Colloids Surf. A* **2015,** *473*, 24-31.

[6] Krueger, A. Carbon nanomaterials. *Beilstein J. Org. Chem.* **2014,** *10*, 1785-1786.

[7] Zabiegaj, D.; Santini, E.; Guzmán, E.; Ferrari, M.; Liggieri, L.; Buscaglia, V.; Buscaglia, M. T.; Battilana, G.; Ravera, F. Nanoparticle laden interfacial layers and application to foams and solid foams. *Colloids Surf. A* **2013,** *438*, 132-140.

[8] Hong, G.; Diao, S.; Antaris, A. L.; Dai, H., Carbon Nanomaterials for Biological Imaging and Nanomedicinal Therapy. *Chem. Rev.* **2015,** *DOI: 10.1021/acs.chemrev.5b00008*.

[9] Beddoes, C. M.; Case, C. P.; Briscoe, W. H. Understanding nanoparticle cellular entry: A physicochemical perspective. *Adv. Colloid Interface Sci.* **2015,** *218*, 48-68.

[10] Kramek-Romanowska, K.; Odziomek, M.; Sosnowski, T. R. Dynamic tensiometry studies on interactions of novel therapeutic inhalable powders with model pulmonary surfactant at the air-water interface. *Colloids Surf. A* **2015,** *480*, 149-158.

[11] Sosnowski, T.R. Nanosized and Nanostructured Particles in Pulmonary Drug Delivery. *J. Nanosci. Nanotechnol.* **2015**, *15*, 3476-3487.

[12] Sosnowski, T. R.; Kolinski, M.; Gradon, L. Interactions of Benzo[a]pyrene and Diesel Exhaust Particulate Matter with the Lung Surfactant System. *Ann. Occup. Hyg.* **2011,** *55*, 329-338.

[13] Colvin, V.L. The potential environmental impact of engineered nanomaterials. *Nat. Biotechnol.* **2003**, *21*, 1166-1170.

[14] Hoet, P. H. M.; Brüske-Hohlfeld, I.; Salata, O. V. Nanoparticles – known and unknown health risks. *J. Nanobiotech.* **2004**, *2*, 12.

[15] Kondej, D.; Sosnowski, T. R. Changes in the Activity of the Pulmonary Surfactant after Contact with Bentonite Nanoclay Particles. *Chem. Eng. Trans.* **2012,** *26*, 531-536.

[16] Harishchandra, R. K.; Saleem, M.; Galla, H.-J., Nanoparticle interaction with model lung surfactant monolayers. *J. Royal Soc. Interface* **2010,** *7*, S15-S27.

[17] Sachan, A. K.; Harishchandra, R. K.; Maskos, C. B. M.; Reichelt, R.; Galla, H.-J. High-Resolution Investigation of Nanoparticle Interaction with a Model Pulmonary Surfactant Monolayer. *ACS Nano* **2012,** *6*, 1677-1687.

[18] Tatur, S.; Badia, A. Influence of Hydrophobic Alkylated Gold Nanoparticles on the Phase Behavior of Monolayers of DPPC and Clinical Lung Surfactant. *Langmuir* **2012,** *28*, 628-639.

[19] Choe, S.; Chang, R.; Jeon, J.; Violi, A. Molecular Dynamics Simulation Study of a Pulmonary Surfactant Film Interacting with a Carbonaceous Nanoparticle. *Biophys. J.* **2010**, *95*, 4102-4114.

[20] Farnoud, A. M.; Fiegel, J. Interaction of Dipalmitoyl Phosphatidylcholine Monolayers with a Particle-laden Subphase. *J. Phys. Chem. B* **2013,** *117,* 12124–12134.

[21] Farnoud, A. M.; Fiegel, J. Low concentrations of negatively charged sub-micron particles alter the microstructure of DPPC at the air–water interface. *Colloids Surf. A* **2012,** *415*, 320– 327.

[22] Daniels, C. B.; Orgeig, S. Pulmonary Surfactant: The Key to the Evolution of Air Breathing. *News Physiol. Sci* **2003,** *18*, 151-157.

[23] Hawgood, S.; Derrick, M.; Poulain, F. Structure and properties of surfactant protein B. *Biochim. Biophys. Acta* **1998,** *1408*, 150-160.

[24] Johansson, J.; Gustafsson, M.; Palmblad, M.; Zaltash, S.; Robertson, B.; Curstedt, T. Synthetic surfactant protein analogues. *Biol. Neonate* **1998,** 74, 9-14.

[25] Zuo, Y.Y.; Veldhuizen, R. A. W.; Neumann, A. W.; Petersen, N. O.; Possmayer, F., Current perspectives in pulmonary surfactant—Inhibition, enhancement and evaluation. *Biochim. Biophys. Acta* **2008,** *1778*, 1947-1977.

[26] Johansson, J.; Curstedt, T.; Robertson, B. The proteins of the surfactant system. *Eur. Resp. J.* **1994,** *7*, 372-391.

[27] Wüstneck, R.; Perez-Gil, J.; Wüstneck, N.; Cruz, A.; Fainerman, V.B.; Pison, U. Interfacial properties of pulmonary surfactant layers. *Adv. Colloid Interface Sci.* **2005**, *117*, 33–58.

[28] Kaganer, V. M.; Mohwald, H.; Dutta, P. Structure and phase transitions in Langmuir monolayers. *Rev. Mod. Phys.* **1999,** *71*, 779-819.

[29] Möhwald, H. Phospholipid and Phospholipid-Protein Monolayers at the Air/Water Interface. *Ann. Rev. Phys. Chem.* **1990,** *41*, 441-476.

[30] Vollhardt, D.; Nandi, N.; Banik, S. D. Nanoaggregate shapes at the air/water interface. *Phys.Chem. Chem. Phys.* **2011,** *13*, 4812-4829.

[31] Giner-Casares, J.J.; Brezesinski, G.; Möhwald, H. Langmuir monolayers as unique physical models. *Curr. Opin. Colloid Interface Sci.* **2014,** *19*, 176-182.

[32] Mendoza, A.J.; Guzmán, E.; Martínez-Pedrero, F.; Ritacco, H.; Rubio, R.G.; Ortega, F.; Starov, V.M; Miller, R. Particle laden fluid interfaces: Dynamics and Interfacial rheology. *Adv. Colloid Interface Sci.* **2014**, *206*, 303-319.

[33] Santini, E.; Guzmán, E.; Ferrari, M.; Liggieri, L. Emulsions stabilized by the interaction of silica nanoparticles and palmitic acid at the water–hexane interface. *Colloids Surf. A* **2014**, *460*, 333-341.

[34] Maestro, A.; Guzmán, E.; Ortega, F.; Rubio, R.G. Contact angle of micro- and nanoparticles at fluid interfaces. *Curr. Opin. Colloid Interface Sci.* **2014**, *19*, 355-367.

[35] Santini, E.; Guzmán, E.; Ravera, F.; Ciajolo, A.; Alfè, M.; Liggieri, L.; Ferrari, M. Soot particles at the aqueous interface and effects on foams stability. *Colloids Surf. A* **2012**,413, 216-223.

[36] Zabiegaj, D.; Santini, E.; Guzmán, E.; Ferrari, M.; Liggieri, L.; Ravera, F. Carbon Soot–Ionic Surfactant Mixed Layers at Water/Air Interfaces. *J. Nanosci. Nanotech.* **2015**, 15, 3618-3625.

[37] Phillips, M. C.; Chapman, D. Monolayer characteristics of saturated 1,2-diacyl phosphatidylcholines (lecithins) and phosphatidylethanolamines at the air-water interface. *Biochim. Biophys. Acta* **1968,** *163*, 301-313.

[38] Klopfer, K. J.; Vanderlick, T. K. Isotherms of Dipalmitoylphosphatidylcholine (DPPC) Monolayers: Features Revealed and Features Obscured. *J. Colloid Interface Sci.* **1996,** *182*, 220-229.

[39] Baldyga, D. D.; Dluhy, R. A. On the use of deuterated phospholipids for infrared spectroscopic studies of monomolecular films: a thermodynamic analysis of single and binary component phospholipid monolayers. *Chem. Phys. Lipids* **1998,** *96*, 81-97.

[40] Wüstneck, R.; Wüstneck, N.; Grigoriev, D. O.; Pison, U.; Miller, R. Stress relaxation behaviour of dipalmitoyl phosphatidylcholine monolayers spread on the surface of a pendant drop. *Colloids Surf. B* **1999,** *15*, 275-288.

[41] Arriaga, L. R.; López-Montero, I.; Ignés-Mullol, J.; Monroy, F. Domain-Growth Kinetic Origin of Nonhorizontal Phase Coexistence Plateaux in Langmuir Monolayers: Compression Rigidity of a Raft-Like Lipid Distribution. *J. Phys. Chem. B* **2010,** *114*, 4509-4520.

[42] Bringezu, F.; Ding, J.; Brezesinski, G.; Zasadzinski, J. A. Changes in Model Lung Surfactant Monolayers Induced by Palmitic Acid. *Langmuir* **2001,** *17*, 4641-4648.

[43] Piknova, B.; Schram, V.; Hall, S. B., Pulmonary surfactant: phase behavior and function. *Curr. Opin. Struct. Biology* **2002**, *12*, 487-494.

[44] Boal, D. H., *Mechanics of the Cell*; Cambridge Univ. Press:Cambridge-United Kingdom, 2002.

[45] Guzmán, E.; Liggieri, L.; Santini, E.; Ferrari, M.; Ravera, F. Effect of Hydrophilic and Hydrophobic Nanoparticles on the Surface Pressure Response of DPPC Monolayers. *J. Phys. Chem. C* **2011**, *115*, 21715–21722.

[46] Wang, Z.; Li, X.; Yang, S. Studies of Dipalmitoylphosphatidylcholine (DPPC) Monolayers Embedded with Endohedral Metallofullerene (Dy@C82). *Langmuir* **2009**, *25*, 12968-12973

[47] Wang, Z.; Yang, S. Effects of Fullerenes on Phospholipid Membranes: A Langmuir Monolayer Study. *ChemPhysChem* **2009**, 10, 2284-2289.

[48] Melbourne, J.; Clancy, A.; Seiffert, J.; Skepper, J.; Tetley, T. D.; Shaffer, M. S. P.; Porter, A., An investigation of the carbon nanotube - Lipid interface and its impact upon pulmonary surfactant lipid function. *Biomaterials* **2015,** *55*, 24-32.

[49] Valle, R. P.; Huang, C. L.; Loo, J. S. C.; Zuo, Y. Y. Increasing Hydrophobicity of Nanoparticles Intensifies Lung Surfactant Film Inhibition and Particle Retention. *ACS Sustainable Chem. Eng.* **2014,** *2*, 1574−1580.

[50] Santini, E.; Ravera, F.; Ferrari, M.; Alfè, M.; Ciajolo, A.; Liggieri, L. Interfacial properties of carbon particulate-laden liquid interfaces and stability of related foams and emulsions. *Colloids Surf. A* **2010**, 365, 189-198.

[51] Hifeda, Y. F.; Rayfield, G. W. Evidence for first-order phase transitions in lipid and fatty acid monolayers. *Langmuir* **1992,** *8*, 197-200.

[52] Hilles, H.; Monroy, F.; Bonales, L. J.; Ortega, F.; Rubio, R. G. Fourier-transform rheology of polymer Langmuir monolayers: Analysis of the non-linear and plastic behaviors. *Adv. Colloid Interfaces Sci.* **2006**, *122*, 67-77.

[53] Monroy, F., Rivillon, S.; Ortega, F.; Rubio, R.G. Dilational rheology of Langmuir polymer monolayers: Poor-solvent conditions. *J. Chem. Phys.* **2001**, *15*, 530-539.

[54] Guzmán, E.; Liggieri, L.; Santini, E.; Ferrari, M.; Ravera, F. Influence of silica nanoparticles on dilational rheology of DPPC–palmitic acid Langmuir monolayers. *Soft Matter* **2012***, 8*, 3938-3948.

[55] Guzmán, E.; Liggieri, L.; Santini, E.; Ferrari, M.; Ravera, F. Mixed DPPC–cholesterol Langmuir monolayers in presence of hydrophilic silica nanoparticles. *Colloids Surf. B* **2013**, *105*, 284-293.

[56] Guzmán, E.; Liggieri, L.; Santini, E.; Ferrari, M.; Ravera, F. Influence of Silica Nanoparticles on Phase Behavior and Structural Properties of DPPC–Palmitic Acid Langmuir Monolayers. *Colloids Surf. A* **2012**, 413, 280-287.

[57] Kretzschmar, G.N.; Li, J.; Miller, R.; Motschmann, H.; Möhwald, H. Characterisation of phospholipid layers at liquid interfaces. 3. Relaxation of spreading phospholipid monolayers under harmonic area changes. *Colloids Surf. A* **1996**,*114*, 277-285.

[58] Weidemann, G.; Vollhardt, D. Long range tilt orientational order in phospholipid monolayers: a comparison of the order in the condensed phases of dimyristoylphosphatidylethanolamine and dipalmitoylphosphatidylcholine. *Colloids Surf. A* **1995**, *100*, 187-202.

[59] Pérez-Gil, J. Structure of pulmonary surfactant membranes and films:The role of proteins and lipid–protein interactions. *Biochim. Biophys. Acta* **2008**, *1778*, 1676-1695.

[60] Lin, X.; Li, Y.; Gu, N. Molecular dynamics simulations of the interactions of charge-neutral PAMAM dendrimers with pulmonary surfactant. *Soft Matter* **2011**, 7, 3882-3888.

[61] Guzmán, E.; Orsi, D.; Liggieri, L.; Cristofolini, L.; Ravera, F. 2D DPPC Based Emulsion–like Structures Stabilized by Silica Nanoparticles. *Langmuir* **2014**, *30*, 11504-11512.

[62] Lee, D. W.; Min, Y.; Dhar, P.; Ramachandran, A.; Israelachvili, J. N.; Zasadzinski, J. A. Relating domain size distribution to line tension and molecular dipole density in model cytoplasmic myelin lipid monolayers. *Proc. Nat. Acad. Sci. U.S.A.* **2011,** *108*, 9425-9430.

[63] Gong, K.; Fheng, S.S.; Go, M.L.; Soew, P.H. Effects of pH on the stability and compressibility of DPPC/cholesterol monolayers at the air–water interface. *Colloids Surf A* **2002**, *207*, 113-125.

[64] Qiao, R.; Roberts, A.P.; Mount, A.S.; Klaine, S.J.; Ke, P.C. Translocation of C60 and Its Derivatives Across a Lipid Bilayer. *Nano Lett.* **2007**, *7*, 614-619

[65] Ma, G.; Allen, H.C. Real-Time Investigation of Lung Surfactant Respreading with Surface Vibrational Spectroscopy. Langmuir **2006**, *22*, 11267-11274

[66] Gómez-Gil, L.; Schürch, D.; Goormaghtigh, E.; Pérez-Gil, J. Pulmonary Surfactant Protein SP-C Counteracts the Deleterious Effects of Cholesterol on the Activity of Surfactant Films under Physiologically Relevant Compression-Expansion Dynamics. *Biophys. J.* **2009,** *97*, 2736-2745.

[67] Lucassen, J.;van den Tempel, M. Dynamical measurements of dila- tional properties of a liquid interface. *Chem. Eng. Sci*. **1972**, *27*, 1283-1291.

[68] Miller, R.; Liggieri, L., *Interfacial Rheology*, Brill:Leiden-The Netherlands, 2009.

[69] Loglio, G.; Tesei, U. ; Cini, R. Surface compressional modulus of surfactant solutions. A time domain method of measurement. *Ber. Bunsen-Ges. Phys. Chem.*, **1977**, 81, 1154-1156.

[70] Ravera, F.; Ferrari, M.; Santini, E.; Liggieri, L. Influence of surface processes on the dilational visco-elasticity of surfactant solutions. *Adv. Colloid Interface Sci.* **2005**, *117*, 75-100.

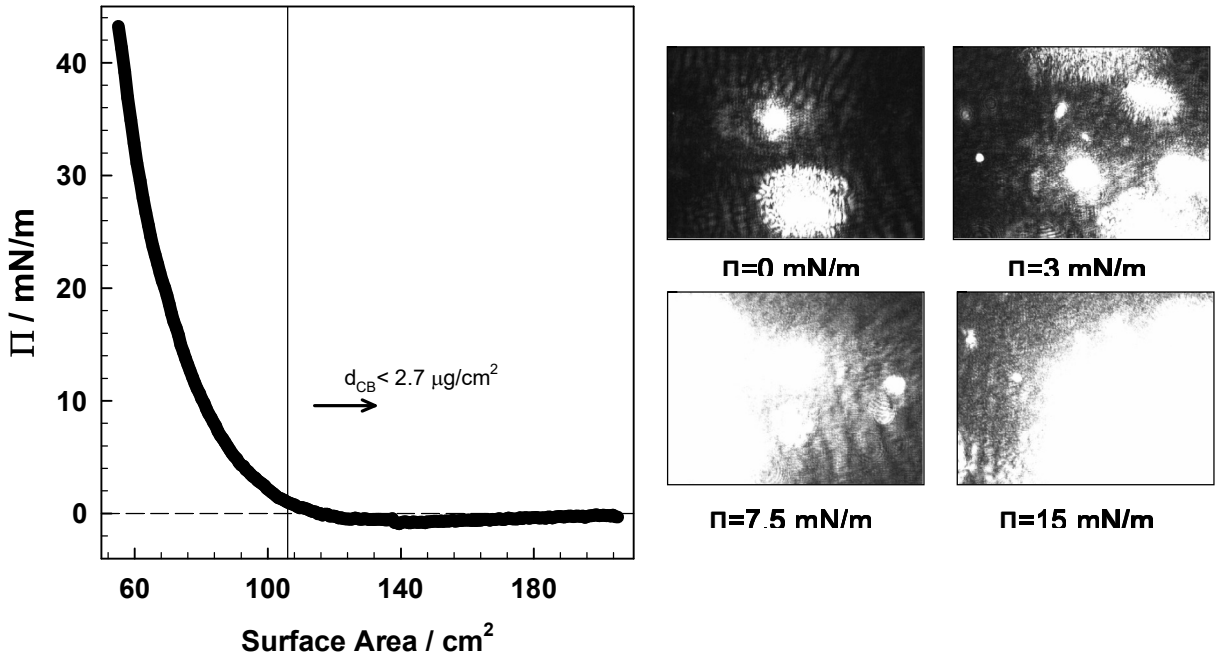

a) **b)**

Figure 1: Compression Surface Pressure – Area isotherm, obtained by the Langmuir trough after the deposition of 0.29 mg of CB particles on pure water (a) and BAM images (size = 311 μm x 418 μm) at different values of surface pressure (b).

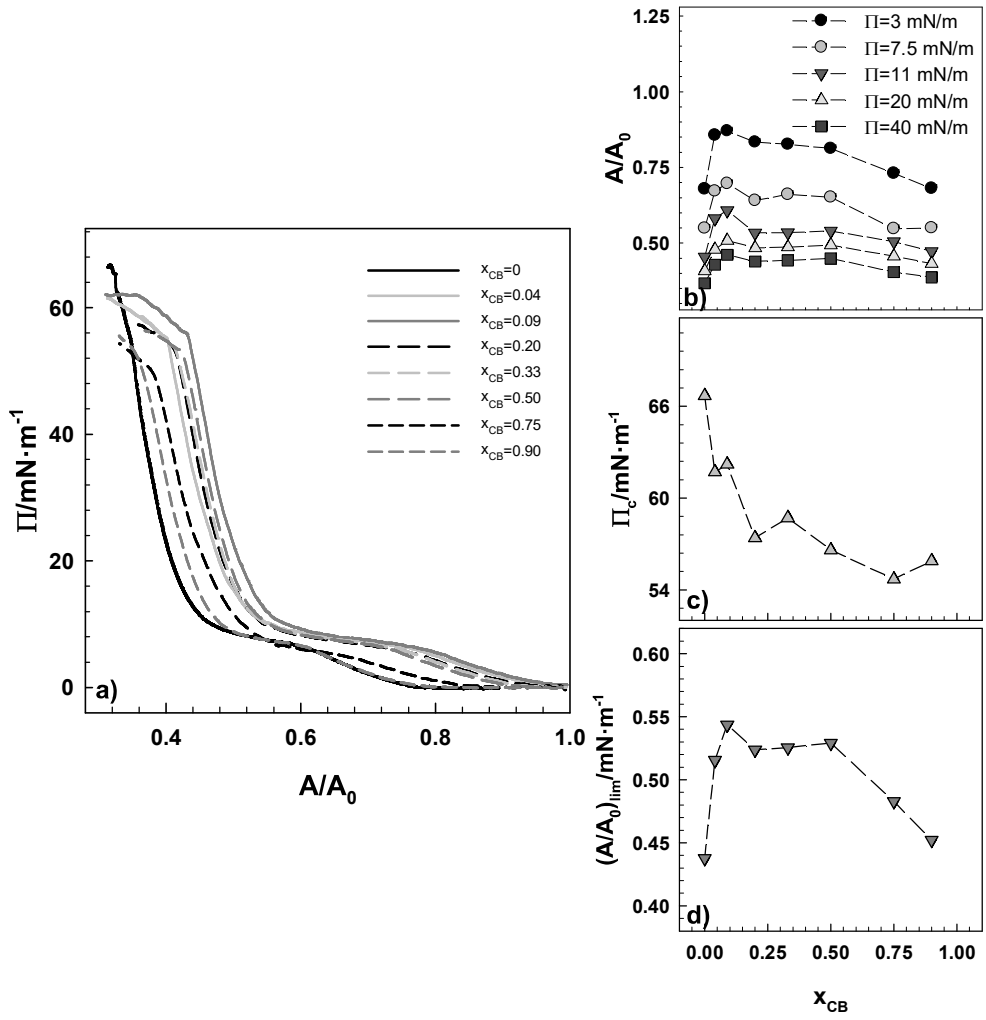

Figure 2. (a) *Π-A/A₀* isotherms of Langmuir monolayer for mixture of DPPC and CB at different weight ratio (a) and dependence on the CB weight fraction, x_{CB}, of A/A_0 at given surface pressure (a), of the collapse pressure, Π_c, (c) and of $(A/A_0)_{lim}$ *(d).*

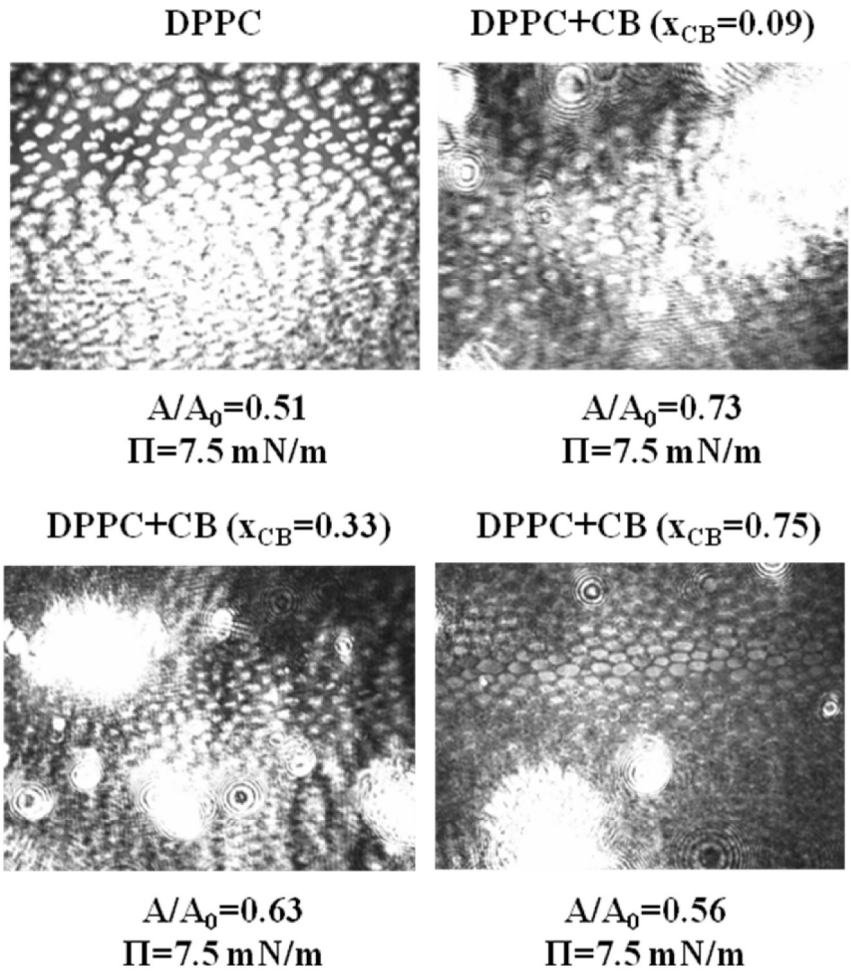

Figure 3. BAM images (size = 311 μm x 418 μm) obtained at *Π=7.5 mN/m,* for mixed DPPC-CB monolayers with different DPPC:CB weight ratio.

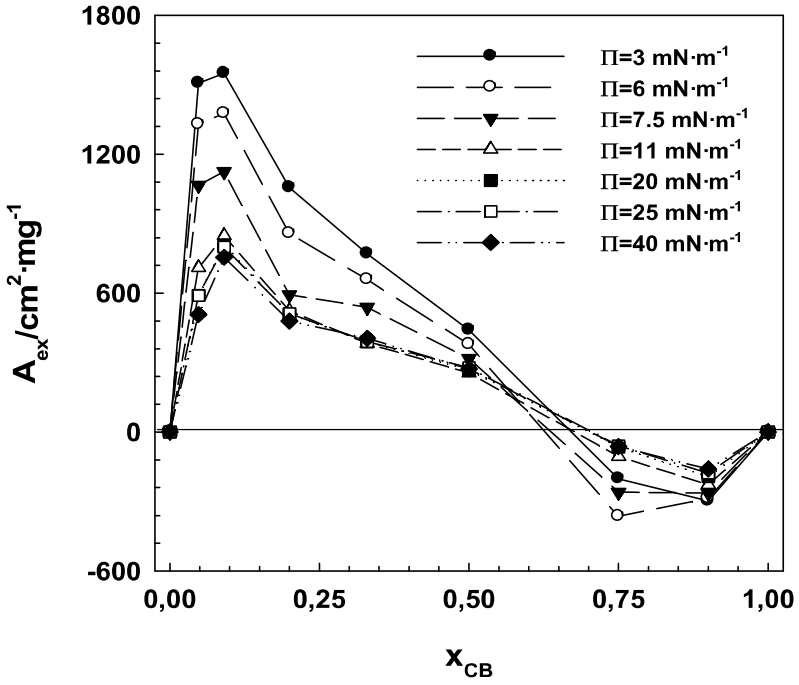

Figure 4. A_{ex} dependence on the x_{CB} for different values of the surface pressures.

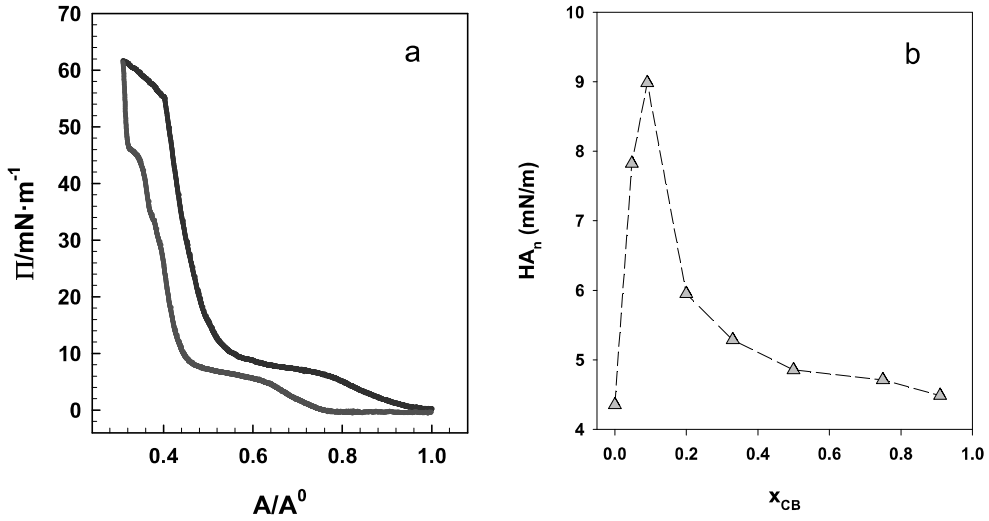

Figure 5. Example of hysteresis cycle obtained for the complete compression – expansion of the mixed DPPC-CB monolayers at x_{CB}=0.04 (a) and calculated Normalised Hysteresis Area versus CB weight fraction.

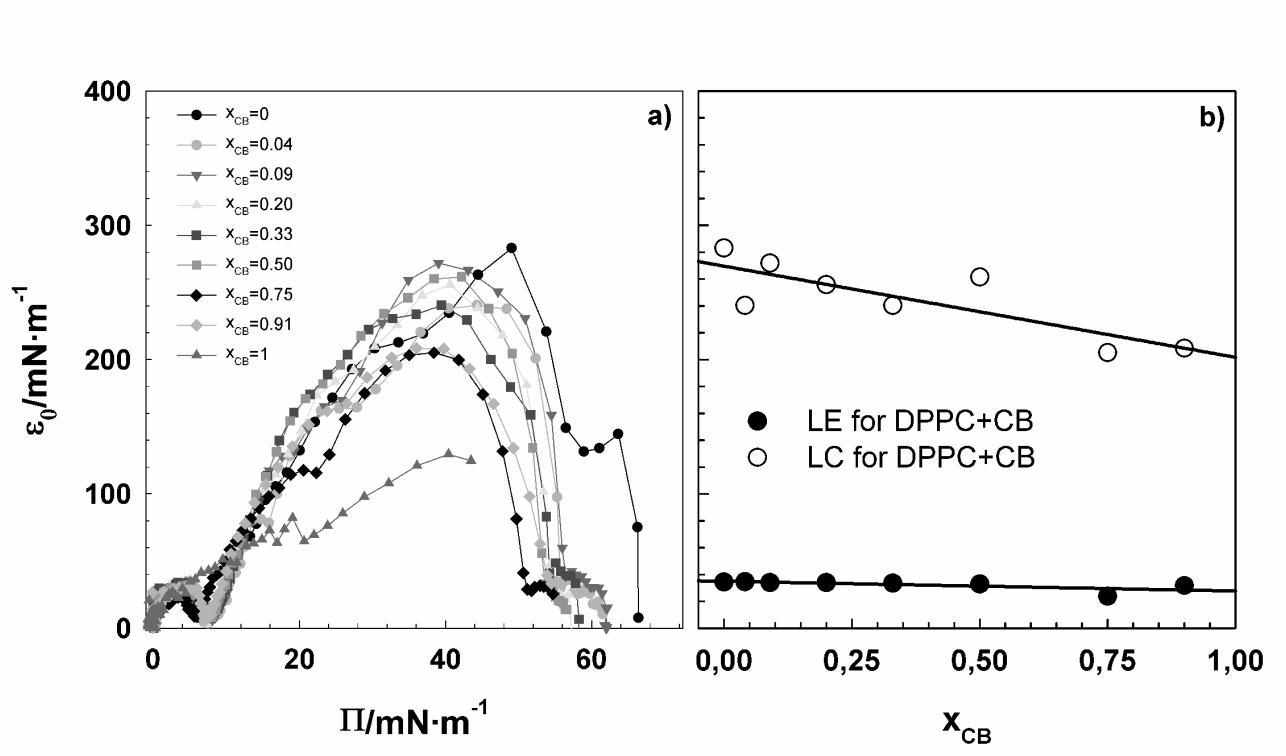

Figure 6. (a) Quasi-equilibrium dilational elasticity calculated from *Π-A* isotherms for the mixed monolayers with different values of x_{CB}. (b) Dependence on x_{CB} of the maximum value of ε_0 for the LE and LC phases.

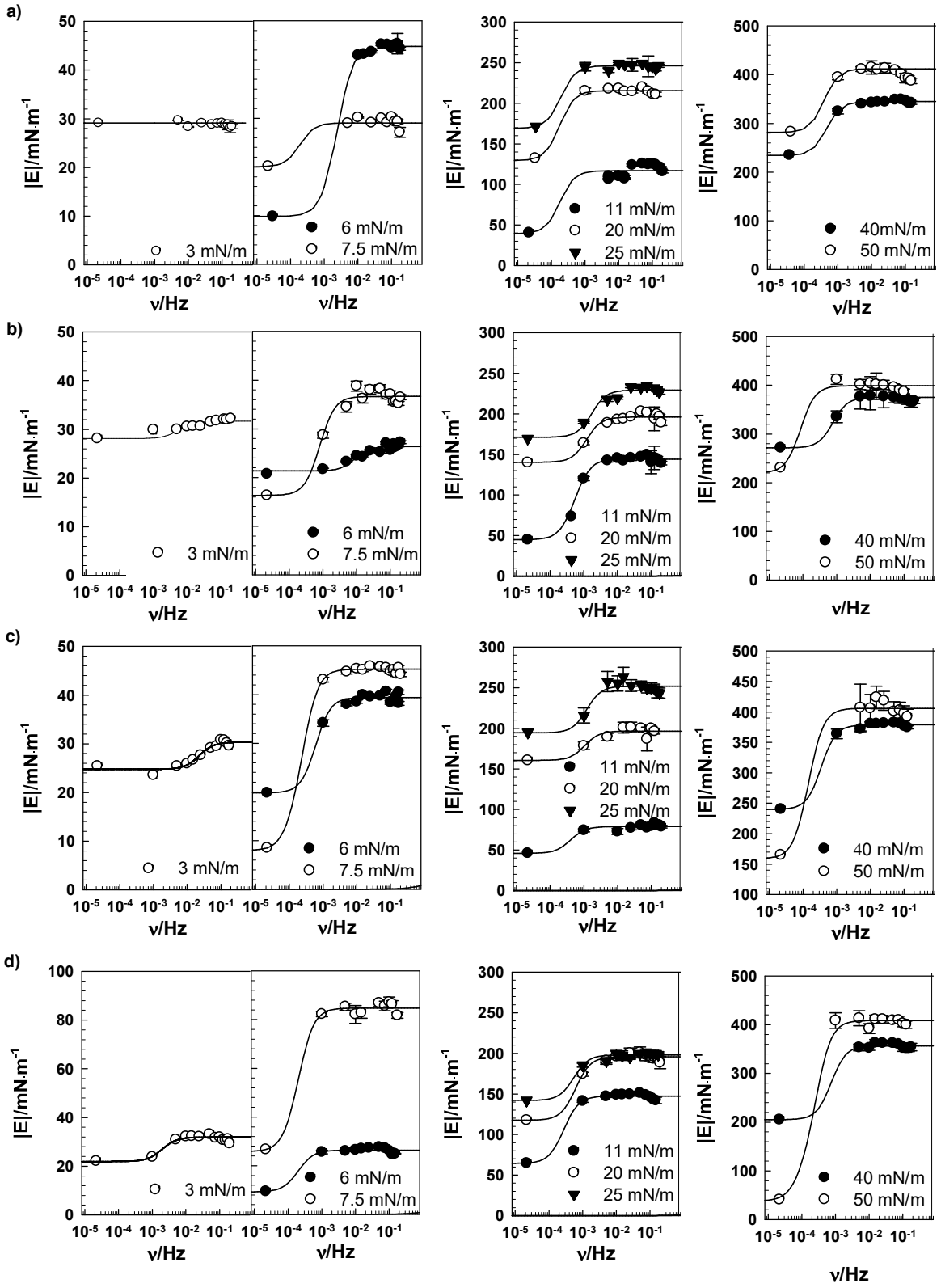

Figure 7. Modulus of the dilational viscoelasticity against frequency obtained by oscillatory barrier experiments for mixed monolayers with different values of x_{CB}, at different values of surface pressure, corresponding to different aggregation states. (a) x_{CB} = 0. (b) x_{CB} = 0.09. (c) x_{CB} = 0.33. (d) x_{CB} = 0.75. Lines represent the best fit theoretical curves according to eq. (5).

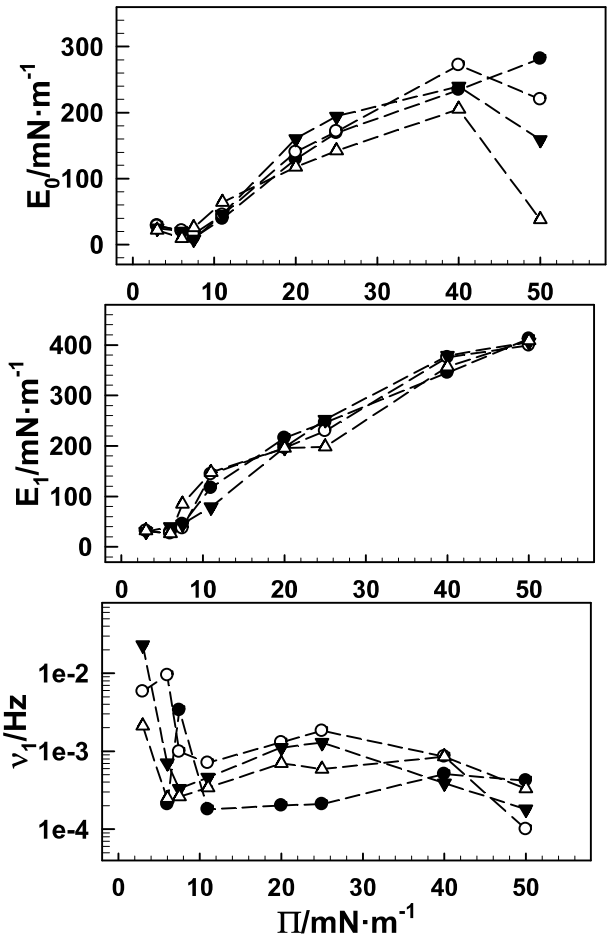

Figure 8. Parameters obtained from the fitting of the rheological experiments of Figure 6 according to eq.(5). The different symbols indicate different values of x_{CB}: (●) x_{CB} = 0. (○) x_{CB} = 0.09. (▼) x_{CB} = 0.33. (Δ) x_{CB} = 0.75.

TOC Graphic